A novel catalytic mechanism for ATP hydrolysis employed by the N- terminal nucleotide-binding domain of Cdr1p, a multidrug ABC transporter of Candida albicans

ARTICLE *in* BIOCHIMICA ET BIOPHYSICA ACTA · JUNE 2008

Impact Factor: 4.66 · DOI: 10.1016/j.bbamem.2008.04.010 · Source: PubMed

6 AUTHORS, INCLUDING:

Sneha Komath
Jawaharlal Nehru University
58 PUBLICATIONS **639** CITATIONS
SEE PROFILE

Rajendra Prasad
University of Delhi
156 PUBLICATIONS **2,540** CITATIONS
SEE PROFILE

Biochimica et Biophysica Acta 1778 (2008) 2143–2153

Contents lists available at ScienceDirect

Biochimica et Biophysica Acta

journal homepage: www.elsevier.com/locate/bbamem

A novel catalytic mechanism for ATP hydrolysis employed by the N-terminal nucleotide-binding domain of Cdr1p, a multidrug ABC transporter of *Candida albicans*

Versha Rai [a], Manisha Gaur [a], Antresh Kumar [a], Sudhanshu Shukla [a], Sneha Sudha Komath [b,*], Rajendra Prasad [a,*]

[a] Membrane Biology Laboratory, School of Life Sciences, Jawaharlal Nehru University, New Delhi—110067, India
[b] Biophysical Chemistry Laboratory, School of Life Sciences, Jawaharlal Nehru University, New Delhi—110067, India

ARTICLE INFO

Article history:
Received 3 January 2008
Received in revised form 9 April 2008
Accepted 21 April 2008
Available online 2 May 2008

Keywords:
ATP binding cassette
ATP hydrolysis
Fluorescence resonance energy transfer
Multidrug resistance
Nucleotide-binding domain

ABSTRACT

Although essentially conserved, the N-terminal nucleotide-binding domain (NBD) of Cdr1p and other fungal transporters has some unique substitutions of amino acids which appear to have functional significance for the drug transporters. We have previously shown that the typical Cys193 in Walker A as well as Trp326 and Asp327 in the Walker B of N-terminal NBD (NBD-512) of Cdr1p has acquired unique roles in ATP binding and hydrolysis. In the present study, we show that due to spatial proximity, fluorescence resonance energy transfer (FRET) takes place between Trp326 of Walker B and MIANS [2-(4-maleimidoanilino) naphthalene-6-sulfonic acid] on Cys193 of Walker A motif. By exploiting FRET, we demonstrate how these critical amino acids are positioned within the nucleotide-binding pocket of NBD-512 to bind and hydrolyze ATP. Our results show that both Mg^{2+} coordination and nucleotide binding contribute to the formation of the active site. The entry of Mg^{2+} into the active site causes the first large conformational change that brings Trp326 and Cys193 in close proximity to each other. We also show that besides Trp326, typical Glu238 in the Q-loop also participates in coordination of Mg^{2+} by NBD-512. A second conformational change is induced when ATP, but not ADP, docks into the pocket. Asn328 does sensing of the γ-phosphate of the substrate in the extended Walker B motif, which is essential for the second conformational change that must necessarily precede ATP hydrolysis. Taken together our results imply that the uniquely placed residues in NBD-512 have acquired critical roles in ATP catalysis, which drives drug extrusion.

1. Introduction

In the human pathogenic yeast *Candida albicans*, overexpression of the drug efflux pump encoding genes *CDR1* and *CDR2* belonging to the ABC [1–7] and *CaMDR1* belonging to MFS family of transporters is one of the principal mechanisms of azole resistance [8–10]. Among ABC transporters, Cdr1p has emerged as a major drug efflux protein involved in azole resistance [6,11]. Thus, Cdr1p has not only acquired significant clinical importance but is also considered an important target in any design of strategies to combat antifungal resistance [12].

Cdr1p, like other members of the ABC superfamily, has four distinct modules: two TMDs consisting of six transmembrane segments and two NBDs located on the cytosolic side of the membrane. The NBDs, which couple energy of ATP hydrolysis to power drug export are highly conserved throughout the evolutionary scale [2,1]. Each NBD contains three characteristic motifs: Walker A and Walker B motifs, which form the nucleotide-binding site [13], and an ABC signature sequence, or C motif, for which several functions have been proposed, including communication between the TMDs and NBDs during the transport cycle [14].

Currently, there is very limited information regarding the structural architecture of NBDs of ABC proteins. For many ABC transporters there is evidence that the two NBDs, although highly similar in sequence, may adopt different functional roles in the transport cycle [15,16]. A high-resolution crystal structure for the NBD subunit of histidine permease (HisP) has its two catalytic sites facing away from each other in the crystal dimer [17]. Jones and George, on the other hand, proposed a model of interaction between the two NBDs in which the Signature motif of one of the NBDs is directly involved in ATP binding by the other and is important for catalysis [18]. A similar

Abbreviations: ABC, ATP binding cassette; MFS, *M*ajor *F*acilitator *S*uperfamily; ATP, adenosine triphosphate; DTE, dithioerythritol; FRET, fluorescence resonance energy transfer; MIANS, 2′-(4′-maleimidylanilino)naphthalene-6-sulfonic acid; NBD, nucleotide-binding domain; TMD, transmembrane domain; NEM, *N*-ethylmaleimide; NBS, *N*-bromosuccinimide

* Corresponding authors. Prasad is to be contacted at Tel.: +91 11 26704509; fax: +91 11 26741081. Komath, Tel.: +91 11 26704502.
E-mail addresses: sskomath@yahoo.com (S.S. Komath), rp47jnu@gmail.com (R. Prasad).

0005-2736/$ – see front matter © 2008 Elsevier B.V. All rights reserved.
doi:10.1016/j.bbamem.2008.04.010

structure was proposed for the catalytic domain of Rad50 [1]. In human P-gp, a close homologue of Cdr1p, the issue of functional asymmetry of the two NBDs remains contentious with proposals both in favor [19,20] and against [21–23] functional asymmetry.

In contrast to most ABC transporters, the NBDs of fungal transporters, including Cdr1p, have unique positioning of a typical Cys193 in Walker A of N-terminal NBDs as well as Trp326 and Asn328 in and adjacent to Walker B motifs, respectively [24]. Thus the otherwise much conserved N-terminal NBDs of fungal transporters have the distinction of unique positioning of typical amino acid residues. On the other hand, the C-terminal NBD of Cdr1p and other ABC fungal transporters possess perfectly conserved motifs, which are essentially identical to those in non-fungal transporters as well [24].

Based on sequence analyses and these unique substitutions, it was earlier suggested that the N-terminal NBD of Pdr5p from *S. cerevisiae* is probably unable to perform ATP hydrolysis and that the transporter might function with only one of its two NBDs [24]. Since Pdr5p is a close homologue of Cdr1p, we expected that such a model, by extension, would be applicable to Cdr1p as well. However, we found that the NBDs in Cdr1p were functionally asymmetric and the swapping of NBDs resulted in non-functional Cdr1p chimeras, suggesting that the two NBDs were essential and non-exchangeable [25]. Further, by purifying the N-terminal NBD of Cdr1p in isolation, and generating several mutants, we have recently shown in a series of papers that not only is this domain capable of ATPase activity, but its unique amino acid substitutions also figure in this functioning.

To begin defining the functional significance of the conserved substitutions in N-terminal NBD of Cdr1p, we demonstrated that replacement of the unique Cys193 with Ala gravely impaired ATP hydrolysis without affecting its ability to bind the nucleotide [26,27]. On the other hand, substitution of Trp326 with Ala resulted only in the loss of ATP binding [28]. Substitution of the highly conserved, putative catalytic residue, Asp327 with Asn yielded a mutant variant protein with strongly impaired ATPase activity but comparable nucleotide binding to that of the wild type protein. Thus Asp327 of Cdr1p, unlike in other non-fungal ABC transporters, is a catalytic base and is unlikely to be involved in Mg^{2+} coordination [28,29]. In each case, we backed up results obtained from domain analysis by making the same mutations in the full-length protein and showing that the mutations actually do have a functional relevance.

The current paper deals with the mechanistic details of how the N-terminal NBD of Cdr1p actually binds and hydrolyzes ATP. Using FRET we show that there are two distinct conformational changes in this domain that correspond to Mg^{2+} coordination and ATP binding, respectively, and which are both important for the subsequent ATP hydrolysis activity.

2. Experimental procedures

2.1. Materials

Disodium-ATP and ADP, NEM and DTE were purchased from Sigma Chemical Co. MIANS was supplied by Molecular Probes.

2.2. Methods

2.2.1. Construction of mutant variant of NBD-512 by site directed mutagenesis

Site directed mutagenesis was performed using the quick-change site directed mutagenesis kit (Stratagene, La Jolla, CA) as described previously [29]. Sequential Cys and Trp mutations and other mutations were introduced into plasmid pSJGN1-8 according to the manufacturer's instructions, and sequentially mutated plasmid was transformed in *E. coli* BL21 (DE3) pLysS cells listed in Table 1. Oligonucleotides used in this study, as listed in Supplementary data Table TS1 were commercially procured from Sigma Genosys, Inc. The presence and authenticity of the desired mutations were confirmed by dideoxy sequencing.

2.2.2. NBD-512 (NBD1) and its mutant variant's purification and measurement of ATPase activity

NBD-512 was purified from SJGN1-8 bacterial strain as described previously [26]. Mg^{2+} dependent ATPase activity of the purified NBD-512 was determined by assessing the release of inorganic phosphate from ATP, as described previously [26] in the presence of 5 mM ATP and 8 mM $MgCl_2$ at 30 °C.

2.2.3. Labeling of purified NBD-512 and its mutant variants with MIANS

To carry out labeling of purified NBD-512, ~50 μg protein was incubated in ATPase buffer (60 mM Tris–Cl pH 6.5 and 8 mM $MgCl_2$) at 22 °C with 50 μM MIANS for 15 min. Unreacted MIANS was quenched with 1 mM DTE. Control unlabelled NBD-512 protein was obtained from the same purified protein preparation. All protein concentrations were adjusted to ~50 μg/ml.

2.2.4. Resonance energy transfer measurements

Fluorescence intensities were measured at 22 °C in a 1 cm-path length cuvette using Cary Eclipse Varian spectrofluorimeter with slit bandwidths of 5 nm for excitation as well as emission. Measured fluorescence intensities were corrected for dilution, for buffer fluorescence, contribution from free and protein-bound MIANS (this was particularly important for Trp emission spectra and is detailed in the next section) and for inner filter effect wherever required. Unless otherwise specified, 1 ml protein samples (0.4 μM) in 60 mM Tris–HCl pH 6.5 containing 8 mM $MgCl_2$ were used for the fluorescence experiments.

2.2.5. Determination of parameters for FRET analysis

The efficiency [E] of resonance energy transfer between the donor and acceptor can be written as $E=1-F/F_o$, where F and F_o are the fluorescence intensities of the donor in the presence and absence of the acceptor, respectively. The spatial distance is given by: $R=R_o\,(E^{-1}-1)^{1/6}$, where R_o is the Förster distance corresponding to 50% energy transfer. R_o was calculated from $R_o=(9.8\times10^3)\,(J\kappa^{k2}Q_Dn^{-4})^{1/6}$ (Å), where J is the spectral overlap integral between donor and acceptor and was determined as in [30,31]; the orientation factor κ^2 was taken as 2/3; Q_D is the fluorescence quantum yield of the donor, and n is the refractive index of the medium, which was taken as 1.33 for dilute aqueous solution [30]. Since MIANS labeling led to a red shift in the emission maximum of Trp fluorescence, we calculated the quantum yield of Trp in MIANS-labelled NBD-512 CW4 (NBD-512 CW4-MIANS) rather than in the unlabelled protein. For this, we corrected the protein emission spectrum for contribution from protein-bound MIANS by obtaining the spectrum of the MIANS-labelled protein after oxidation of its Trp residue using NBS

Table 1
List of strains used in this study

Name	Description	Phenotype
SJGN1-8P	BL21(DE)pLysS cells carrying the pSJGN1-8 plasmid	Wild type functional and active
VRGN W326A	SJGN1-8P cells carrying the pVRGN W326A plasmid	Decrease in ATP binding but can hydrolyze ATP with high K_M and V_{max} values
VRGN D327A	SJGN1-8P cells carrying the pVRGN D327A plasmid	Loss in ATP hydrolysis
VRGN D327N	SJGN1-8P cells carrying the pVRGN D327N plasmid	Loss in ATP hydrolysis
VRGN CW4	SJGN1-8P cells carrying the pVRGN CW4 plasmid	Functional like wild type
VRGN E238A	SJGN1-8P cells carrying the pVRGN E238A plasmid	Decrease in ATP binding but can hydrolyze ATP with high K_M and V_{max} values
VRGN E238Q	SJGN1-8P cells carrying the pVRGN E238Q plasmid	Functional albeit to a moderate level
VRGN E238D	SJGN1-8P cells carrying the pVRGN E238D plasmid	Functional albeit to a moderate level
VRGN N328E	SJGN1-8P cells carrying the pVRGN N328E plasmid	Loss in ATP hydrolysis
VRGN N328A	SJGN1-8P cells carrying the pVRGN N328A plasmid	Loss in ATP hydrolysis
SJGN C193A	SJGN1-8P cells carrying the pSJGN mutC plasmid	Loss in ATP hydrolysis
VRGN C193S	SJGN1-8P cells carrying the pVRGN C193S plasmid	Loss in ATP hydrolysis but can hydrolyze ATP at high pH
VRGN CW4 N328A	SJGN1-8P cells carrying the pVRGN CW4 N328A plasmid	Loss in ATP hydrolysis
VRGN CW4 D327N	SJGN1-8P cells carrying the pVRGN CW4 D327N plasmid	Loss in ATP hydrolysis
VRGN CW4 D327A	SJGN1-8P cells carrying the pVRGN CW4 D327A plasmid	Loss in ATP hydrolysis
VRGN CW4 E238A	SJGN1-8P cells carrying the pVRGN CW4 E238A plasmid	Decrease in ATP binding can hydrolyze ATP with high K_M and V_{max} values

[32]. We also corrected for contribution from NBS alone in the same buffer background. The quantum yield Q_D, of Trp in NBD-512 CW4-MIANS was determined relative to a standard, quinine sulphate (QS). The Trp emission of the labelled protein and QS in 0.1 N H_2SO_4 were measured upon excitation at 295 nm. Both the sample and the standard had the same absorbance (0.1) at 295 nm. The Q_D of NBD-512 CW4-MIANS was calculated using the equation: $Q_D = Q_{NBD\text{-}512\ CW4\text{-}MIANS} = Q_{QS} \times F_{NBD\text{-}512\ CW4\text{-}MIANS} / F_{QS}$, where Q_{QS}, the quantum yield of quinine sulphate, was taken to be 0.51 in 0.1 N H_2SO_4 [30] and $F_{NBD\text{-}512\ CW4\text{-}MIANS}$ and F_{QS} are the integrals of the spectra of NBD-512 CW4-MIANS and QS, respectively, in the range of 310–500 nm. Estimated FRET parameters are listed in Supplementary data Table TS2.

3. Results

Based on previous results, we hypothesized a model for ATP hydrolysis by the N-terminal NBD (NBD-512) of Cdr1p involving the role of typically placed residues such as Cys193 in Walker A as well as Trp326, Asp327 and Asn328 in the Walker B and extended Walker B motifs [29]. The conserved motifs and location of these typical amino acids within them are shown in Fig. 1. However, so far experimental data was insufficient to suggest how these residues are placed with respect to one another for binding and hydrolysis of ATP. To this end, in the present study, we exploited FRET between critical residues of NBD-512. The assumption was that if Trp326 and Cys193 are in close proximity to bind and hydrolyze ATP, respectively, one should be able to monitor FRET between them by fluorescently labeling Cys193. The role of other conserved residues could also be studied by monitoring the effect of their substitution mutations on this FRET.

Due to the fact that NBD-512 possesses four additional Trp and Cys residues and to avoid complications in interpretation of the FRET data, we generated a mutant variant of NBD-512 (designated as NBD-512 CW4) in which all Cys and Trp residues with the exception of Cys193 and Trp326 were replaced with Ala. Having determined that NBD-512 CW4 bound ATP (K_d 0.072±0.04 mM) and hydrolyzed it (K_M 0.185±0.04 mM, V_{max} 80±5 nmol/min/mg) in a manner comparable to NBD-512, we used this mutant variant for further studies.

3.1. MIANS can selectively label Cys193 of NBD-512 CW4 mutant variant

MIANS selectively and covalently modifies cysteine side chains under appropriate conditions and becomes highly fluorescent upon binding to proteins [30,31]. The purified N-terminal NBD (NBD-512) of Cdr1p has five Cys residues that could potentially react with MIANS. Expectedly, the addition of MIANS to purified wild type NBD-512 led to a rapid increase in the fluorescence intensity at 450 nm in a concentration dependent manner (Fig. 2A). Pretreatment of NBD-512 with NEM (another Cys modifying agent) caused no further increase in fluorescence upon addition of MIANS, indicating that the two agents compete for the same site(s) (data not shown).

When MIANS labeling was done with NBD-512 CW4, one could specifically label Cys193. Similar to the wild type NBD-512, an increase in the MIANS fluorescence is observed in this mutant variant, albeit to a lesser extent (Fig. 2C).

Since we know from our previous study that Cys193 is critical for ATP hydrolysis we expected that the presence of ATP prior to MIANS labeling will physically block the access of the fluorophore (Supplementary data Fig. S1). A short pre-incubation with ATP resulted in reduction in the extent of modification of NBD-512 with MIANS (Fig. 2B). There was practically no labeling with MIANS if NBD-512 CW4 was pre-equilibrated with ATP (Fig. 2D). The importance of Cys193 in ATP catalysis was further evident when MIANS labeling was done with NBD-512 C193A mutant variant in which Cys193 was mutated to Ala. It was observed that MIANS could label the other cysteines of NBD-512 C193A mutant variant, even after pretreatment with ATP (Fig. 2E and F). These observations confirmed that modification by MIANS at Cys193 was specifically susceptible to the presence of ATP.

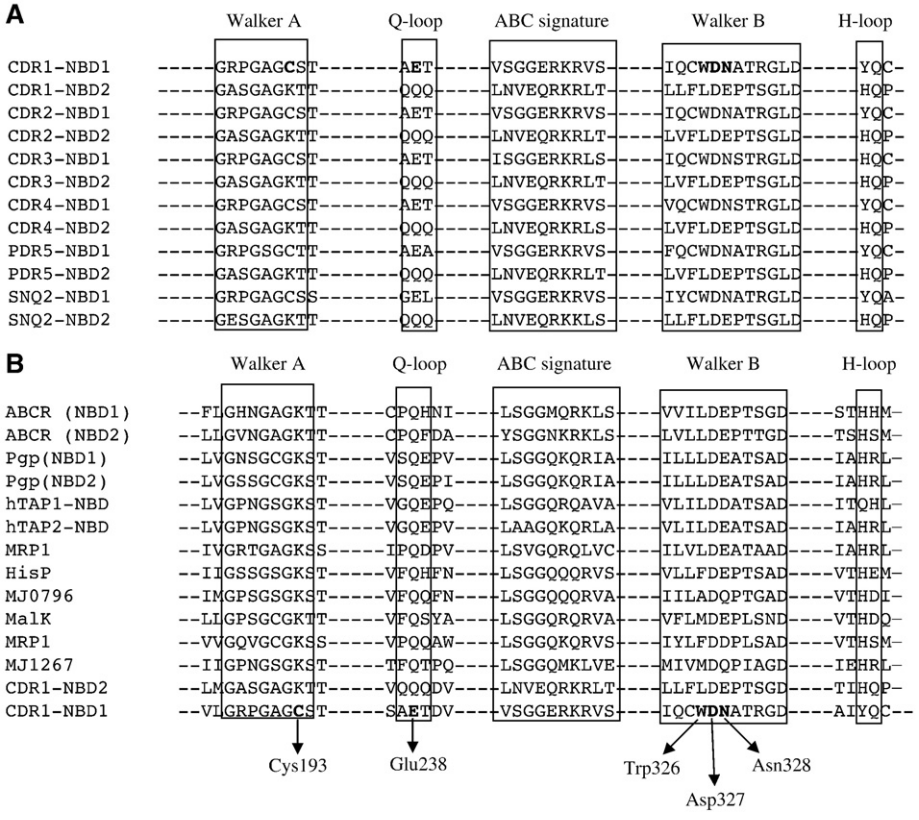

Fig. 1. Sequence alignment of the conserved motifs from fungal ABC transporters. Comparison of the sequence alignment of the Walker A, Q-loop, signature C, Walker B and H-loop motifs of N- and C-terminal NBD of Cdr1p with known (A) Fungal and (B) Non-fungal ABC transporters. Conserved but unique residues Cys193, Glu238, Trp326, Asp327 and Asn328 of N-terminal NBD are marked.

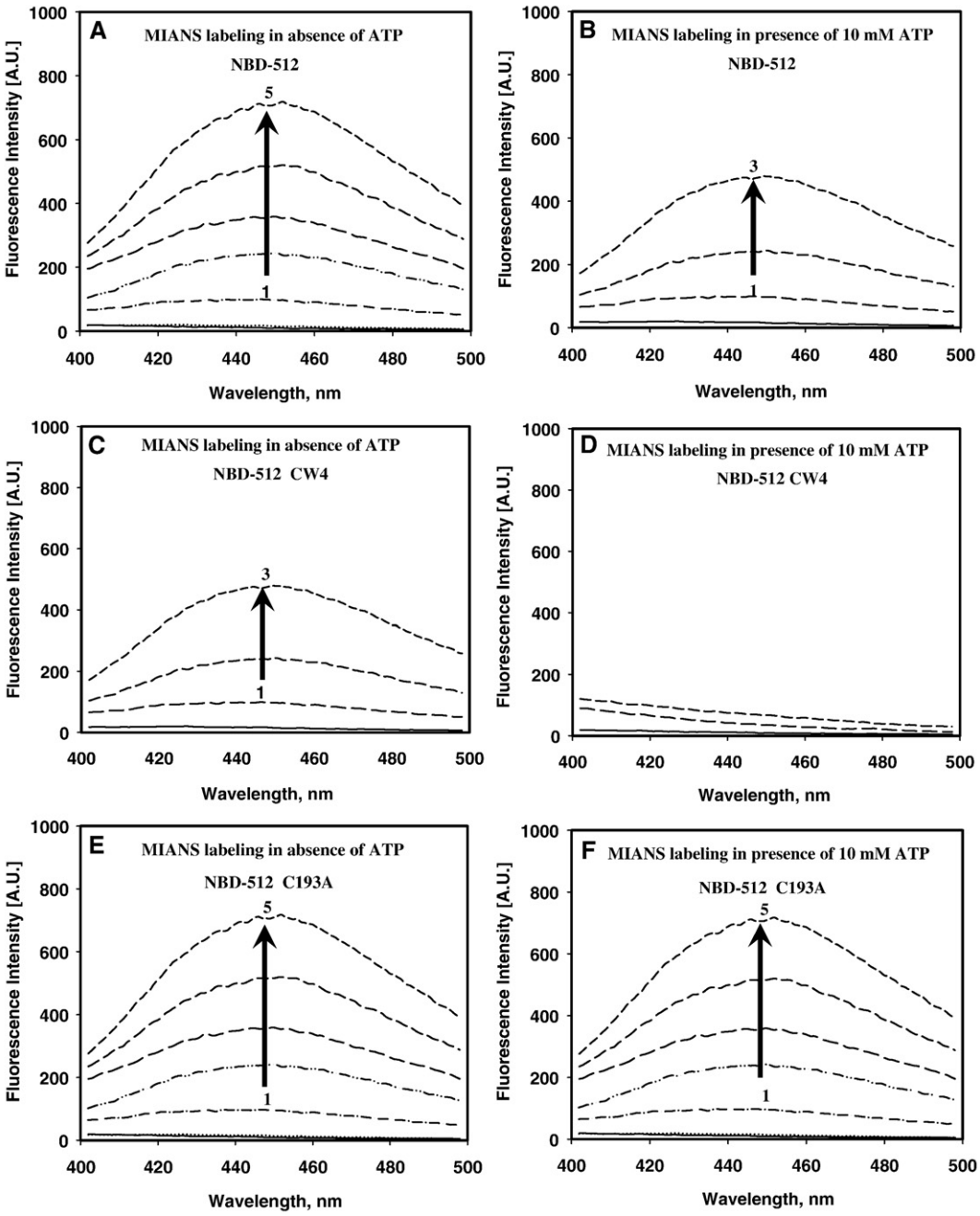

Fig. 2. Fluorescence emission spectra of MIANS-labelled NBD-512, and the effect of ATP on labeling. Samples containing 0.4 μM protein samples in ATPase buffer were excited at 322 nm. Emission spectra were recorded between 400 and 500 nm. Fluorescence emission spectra of NBD-512 and its mutant variant were measured in presence of increasing concentrations of MIANS (curve 1 (1.0 μM), curve 2 (5.0 μM), curve 3 (10 μM), curve 4 (25 μM) and curve 5 (50 μM)). In the presence of 10 mM ATP, partial protection of Cys residues of NBD-512, complete protection of Cys193 in NBD-512 CW4 and no protection of Cys residues of NBD-512 C193A mutant variants from modification by MIANS were observed. Fluorescence spectrum upon MIANS labeling (A) in the absence of ATP with NBD-512 (B) after pre-incubation of NBD-512 with 10 mM ATP (C) in the absence of ATP with NBD-512 CW4 mutant variant (D) after pre-incubation of NBD-512 CW4 mutant variant with 10 mM ATP (E) in the absence of ATP with NBD-512 C193A mutant variant and (F) after pre-incubation of NBD-512 C193A mutant variant with 10 mM ATP.

3.2. MIANS-labelled Cys193 continues to sense ATP docking in the active site

MIANS labeling results in ~5 nm red shifted emission for Trp326 in NBD-512 CW4-MIANS, suggesting that the probe does perturb the nucleotide-binding pocket of the protein. However, our results show that both NBD-512-MIANS and NBD-512 CW4-MIANS continue to sense Mg–ATP docking, exhibiting a concentration dependent, saturable quenching of MIANS fluorescence upon titration with Mg–ATP (Fig. 3A and B). The K_d for Mg–ATP binding to NBD-512-MIANS as well as NBD-512 CW4-MIANS was effectively unaltered (Fig. 3C) [28]. Very similar K_d values were obtained upon titration with Mg–ADP as well (NBD-512-MIANS, 0.07 ± 0.03 mM; NBD-512 CW4-MIANS, 0.07 ± 0.04 mM). Thus, it was possible to extrapolate the information from ATP binding to NBD-512 CW4-MIANS to understand how NBD-512 might function. Of note, ATP caused no shift in MIANS emission maximum in NBD-512-MIANS or NBD-512 CW4-MIANS, indicating that the polarity of the environment around MIANS in either variants remained effectively unaltered.

3.3. Energy transfer occurs between Trp326 and MIANS-labelled Cys193

The fluorescence emission spectrum of Trp326 has a significant degree of overlap with the absorption spectrum of MIANS (λ_{ex}, λ_{em} for tryptophan is 295 and 340 nm; λ_{ex}, λ_{em} for MIANS is 322 and 450 nm).

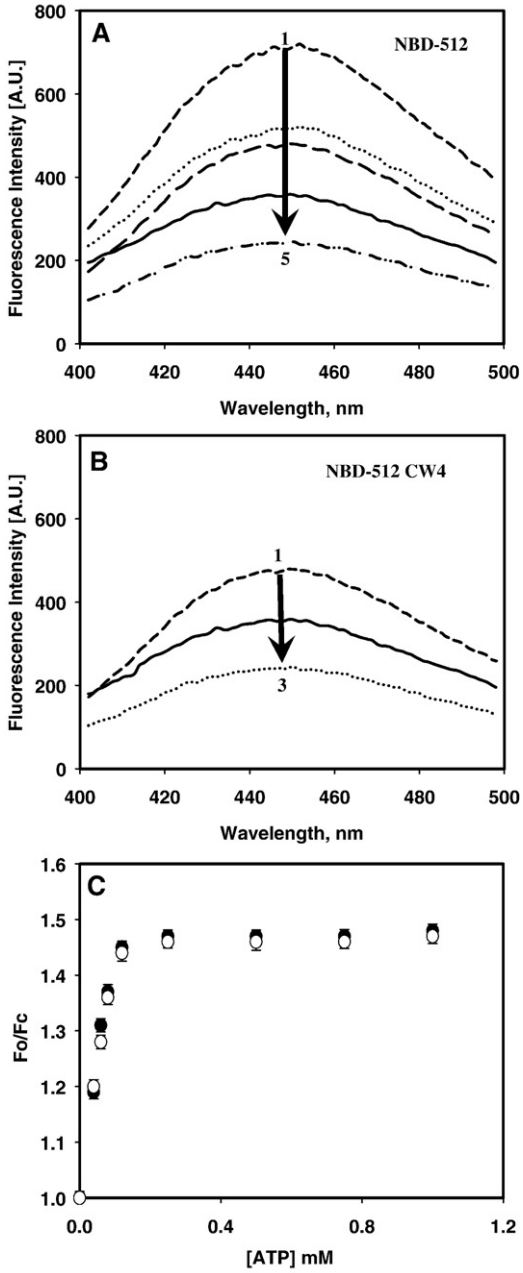

Fig. 3. ATP binding with MIANS-labelled NBD-512 and its mutant variant NBD-512 CW4 monitoring extrinsic MIANS fluorescence. To achieve complete labeling, samples containing 0.4 μM protein in ATPase buffer were incubated with 50 μM MIANS for 15 min. Fluorescence spectra were recorded upon excitation at 322 nm and emission was recorded between 400 and 500 nm. (A) Fluorescence emission spectra of MIANS-labelled NBD-512 in presence of increasing concentrations of ATP (curve 1, no ATP; curve 2, 0.05 mM; curve 3, 0.2 mM; curve 4, 0.5 mM; curve 5, 1.0 mM). (B) Fluorescence emission spectra of MIANS-labelled NBD-512 CW4 mutant variant measured in presence of increasing concentrations of ATP (curve 1, no ATP; curve 2, 0.5 mM; curve 3, 1.0 mM). (C) Concentration dependent binding of ATP to the MIANS-labelled NBD-512 (●) and its mutant variant NBD-512 CW4 (○). Normalized fluorescence intensity (F_o/F_c) was plotted as a function of ATP concentration, where F_o refers to the fluorescence intensity of the sample in absence of ATP and F_c represents the fluorescence emission intensity at 450 nm upon ATP addition (background corrections as mentioned under Methods). The plot represents averages of three different experiments done in duplicates. The bars represent standard deviations. From the slope and ordinate of the Scatchard plot (plot not shown), dissociation constant (K_d) for ATP binding was determined to be 0.07 ± 0.03 mM for NBD-512 and 0.08 ± 0.04 mM for NBD-512 CW4 assuming a single binding site per molecule.

Hence, it is possible to monitor the spatial proximity between the two using FRET. Since MIANS could label Cys193 of NBD-512 CW4, it could form a donor–acceptor pair with Trp326 provided the fluorophores lay within close proximity to each other. To test this, purified NBD-512 and NBD-512 CW4, in a buffer containing Mg^{2+}, were separately excited at 295 nm in the presence of increasing concentrations of MIANS, and fluorescence emission recorded between 310–500 nm (Fig. 4A and B, respectively). We observed a sharp increase in fluorescence emission of protein-bound MIANS at 450 nm; the fluorescence emission of Trp at 340 nm was simultaneously quenched. This effect, due to resonance energy transfer, was concentration dependent.

Trp emission was also ~5 nm red shifted, suggesting that Trp326 in NBD-512 CW4 becomes more solvent-exposed upon incorporation of MIANS. Hence, to obtain reliable estimates of Förster's radius and spatial distances between the two fluorophores, it was important to differentiate between quenching as a result of change in polarity of the environment around Trp from that due to FRET [Supplementary data Table TS2]. For this purpose, we subtracted from the emission spectrum of NBD-512 CW4-MIANS a spectrum of the protein after treatment with NBS as described under Methods. The resultant spectrum was taken as that of Trp326 alone in NBD-512 CW4-MIANS.

3.4. FRET monitors conformational changes induced by Mg^{2+}

We showed previously that Mg–ATP causes a significant conformational change in NBD-512 [28]. However, whether the conformational changes were the result of metal ion coordination or due to nucleotide docking was not apparent from that study [28]. By exploiting FRET and NBD-512 CW4 mutant variant, we re-addressed this issue. Interestingly, in the presence of EDTA and no Mg^{2+}, poor FRET was seen in NBD-512 CW4 upon titration with MIANS (Fig. 5A). MIANS on Cys193 of NBD-512 CW4 was estimated to be at a distance of ~25 Å from Trp326 in the presence of EDTA (Table 2).

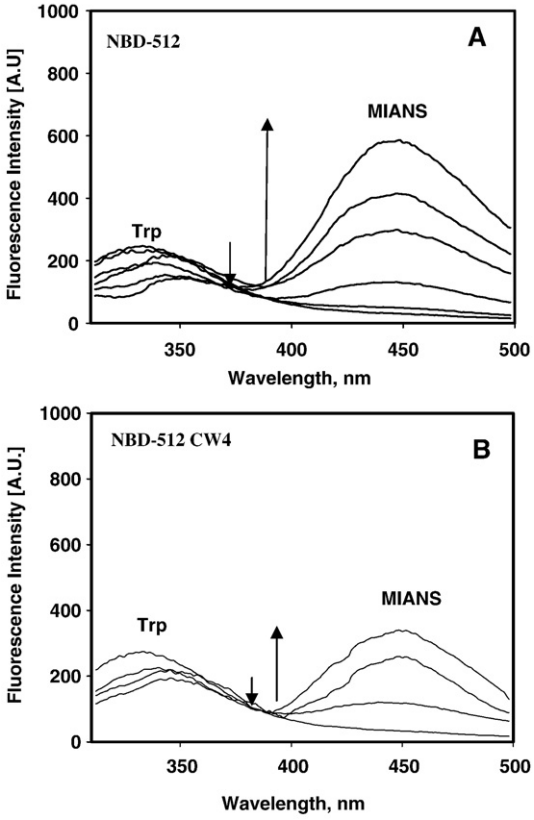

Fig. 4. Fluorescence resonance energy transfer between the donor (Trp) and acceptor (MIANS) in NBD-512 and NBD-512 CW4. Purified 0.4 μM NBD-512 (A) or NBD-512 CW4 (B) mutant variant in ATPase buffer was titrated with increasing concentrations of MIANS (0–50 μM), incubated for 2 min after addition of each aliquot and emission spectra recorded between 310 and 500 nm.

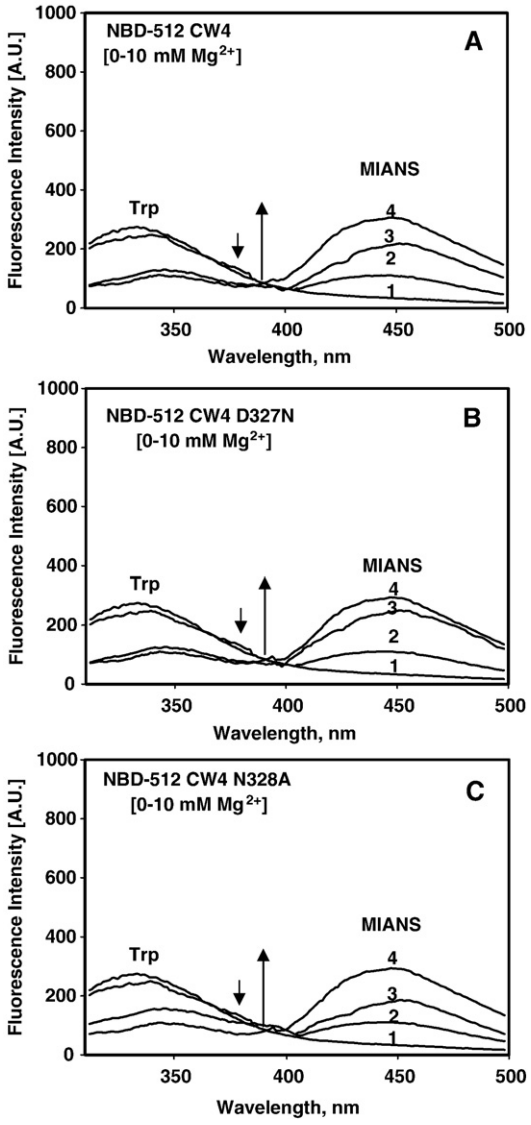

Fig. 5. Effect of Mg^{2+} ion on FRET. Purified 0.4 μM NBD-512 CW4 or mutant variants in Mg^{2+} free ATPase buffer (60 mM Tris–Cl pH 6.5) were incubated with 50 μM MIANS for 15 min. After labeling, the samples were titrated with increasing concentrations of $MgCl_2$ (0–10 mM) and emission spectra were recorded between 310 and 500 nm upon excitation at 295 nm. (A) Fluorescence emission spectra of NBD-512 CW4-MIANS mutant variant in presence of increasing concentrations of $MgCl_2$ (curve 1, unlabelled protein, curve 2, no $MgCl_2$ with 8 mM EDTA; curve 3, 5 mM $MgCl_2$; curve 4, 10 mM $MgCl_2$). (B) Fluorescence emission spectra of MIANS-labelled NBD-512 CW4 D327N mutant variant in presence of increasing concentrations of $MgCl_2$ (curve 1, unlabelled protein, curve 2, no $MgCl_2$ with 8 mM EDTA; curve 3, 7.5 mM $MgCl_2$; curve 4, 10 mM $MgCl_2$). (C) Fluorescence emission spectra of MIANS-labelled NBD-512 CW4 N328A mutant variant in presence of increasing fractions of $MgCl_2$ (curve 1, unlabelled protein, curve 2, no $MgCl_2$ with 8 mM EDTA; curve 3, 3 mM $MgCl_2$; curve 4, 10 mM $MgCl_2$). Efficiencies of Energy transfer were calculated for the change in fluorescence from curve 2 to curve 4 in each case.

Addition of Mg^{2+}, leads to increased FRET and an enhancement of MIANS fluorescence in NBD-512 CW4 (Fig. 5A; Table 2). This further confirms that Trp326 and MIANS on Cys193 arrive within greater spatial proximity (18.2 Å) once Mg^{2+} is coordinated within the nucleotide-binding pocket. That such a conformational change is essential for ATP hydrolysis is clear since the domain is incapable of catalysis in the absence of the metal ion [26,28]. Further, addition of ATP in the absence of the metal ion could not cause any significant effect on FRET, suggesting that binding of Mg^{2+} was a prerequisite for ATP binding. It may also be noted that Mg^{2+} did not affect the fluorescence of MIANS itself in NBD-512 CW4 (data not shown). Hence, it appears unlikely that Cys193 has a direct role in Mg^{2+} coordination.

We had earlier observed that NBD-512 C193A mutant variant binds ATP in a manner similar to wild type and has similar degrees of accessibility to small molecular weight fluorescence quenchers [28]. The K_d for ATP calculated from changes in fluorescence of NBD-512 CW4-MIANS also supports this contention that the protein can bind Mg–ATP even when the Cys193 is labelled by MIANS (Fig. 3C).

It should be pointed out that the probe led to a slight perturbation of the pocket. This, along with the fact that the probe itself is roughly 10 Å in length [31] implies that the distances estimated here should not be taken as the exact spatial distance between Trp326 and Cys193 in the unlabelled protein. Notwithstanding this, the estimated distances between the two fluorophores certainly provide a useful handle for monitoring conformational changes occurring upon ligand binding.

Of note, we observed that another mutant variant, NBD-512 CW4 D327N, crippled in ATP hydrolysis showed conformational change and FRET similar to NBD-512 CW4 when titrated with Mg^{2+} (Fig. 5B). NBD-512 CW4 D327A too behaved very much like NBD-512 CW4 D327N (Supplementary data Fig. S2). This reconfirmed our previous results that the conserved Asp at position 327, unlike its conventional role, does not participate in metal ion coordination (Table 2). Likewise, the catalytically deficient mutant variant NBD-512 CW4 N328A too exhibited FRET comparable to NBD-512 CW4 mutant variant with Mg^{2+} (Fig. 5C; Table 2), suggesting that Asn328 also had no direct role in Mg^{2+} coordination.

3.5. Glu238 also coordinates Mg^{2+}

Because of the unique placements of residues such as Cys193, Trp326, Asp327 and Asn328 in N-terminal NBD of Cdr1p, it appears that the conventional residues are not involved in Mg^{2+} coordination. We already knew that the abstraction of metal ion directly affects the fluorescence spectrum of Trp in NBD-512 [28]. Titration with Mg^{2+}, results in an enhancement of the Trp fluorescence intensity for NBD-512 [28] as well as for NBD-512 CW4 (data not shown). Thus, Trp326 itself appears to be important for Mg^{2+} coordination and the consequent conformational change in NBD-512. Yet all our previous as well as current FRET results indicate that Trp326 alone cannot be responsible for Mg^{2+} coordination. Results from other NBDs of ABC transporters indicate that the commonly occurring glutamine of Q-loop plays an important role either in contacting the γ-phosphate or in interdomain communication [33,34]. In ButCD the conserved Gln in the Q-loop (Gln80) has also been shown to be involved in metal ion coordination [35].

Table 2
Summary of parameters obtained from FRET for NBD-512 CW4 and its mutant variants

NBD-512 mutant variants	Conditions	Average spatial distance [*R*]	% Efficiency of energy transfer [*E*]
NBD-512 CW4	No $MgCl_2$	24.5 Å	20.0±2.5
NBD-512 CW4	10 mM $MgCl_2$	18.2 Å	60.0±1.2
NBD-512 CW4	5 mM Mg–ATP	11.9 Å	95.0±1.2
NBD-512 CW4	5 mM Mg–ADP	14.1 Å	85±1.8
NBD-512 CW4 D327N	No $MgCl_2$	25.1 Å	18±2.1
NBD-512 CW4 D327N	10 mM $MgCl_2$	18.4 Å	58.0±1.4
NBD-512 CW4 D327N	5 mM Mg–ATP	12.1 Å	94.5±1.1
NBD-512 CW4 D327N	5 mM Mg–ADP	14.9 Å	83.2±1.0
NBD-512 CW4 E238A	No $MgCl_2$	24.8 Å	20±1.9
NBD-512 CW4 E238A	10 mM $MgCl_2$	19.7 Å	48.0±1.0
NBD-512 CW4 E238A	5 mM Mg–ATP	17.5 Å	65.0±1.7
NBD-512 CW4 E238A	5 mM Mg–ADP	17.7 Å	64.0±1.8
NBD-512 CW4 N328A	No $MgCl_2$	24.2 Å	19±1.9
NBD-512 CW4 N328A	10 mM $MgCl_2$	18.0 Å	61.1±1.0
NBD-512 CW4 N328A	5 mM Mg–ATP	14.4 Å	86.0±1.5
NBD-512 CW4 N328A	5 mM Mg–ADP	14.4 Å	85.6±1.5

Mg^{2+} was added prior to ATP/ADP addition. No nucleotide binding was seen in the absence of Mg^{2+} as discussed in the text.

The conserved Q-loop of NBD-512 has Glu238 replacing Gln and is a typical substitution for all fungal transporters (Fig. 1). As expected, mutant variants NBD-512 E238A and NBD-512 CW4 E238A were impaired in ATP binding as well as ATPase activity (Fig. 6A and B). Further, FRET analysis showed that this protein underwent a lesser than expected conformational change upon Mg^{2+} addition (Fig. 6C; Table 2). Thus, the mutation of Glu238 specifically impaired the ability of the protein to sense the metal ion. It may be mentioned here that, since Trp326 is intact, metal ion coordination is diminished but not abolished and hence some FRET is expected in this mutant variant.

Replacement with a residue capable of metal ion coordination, as in NBD-512 E238Q and NBD-512 E238D allowed Mg^{2+}-ATP binding in a manner comparable to NBD-512 and NBD-512 CW4 proteins [K_d for NBD-512 E238Q was 0.08 ± 0.01 mM and NBD-512 E238D was 0.07 ± 0.01 mM]. Thus, the uncommon Glu238, is also involved in Mg^{2+} coordination.

Of note, the loss of activity in some of the mutant variants of NBD-512 was not due to their inability to form homodimer; our results show that NBD-512 is a monomer in solution (Supplementary data Fig. S3).

3.6. ATP docking subsequent to Mg^{2+} coordination induces further conformational changes

Having shown that Mg^{2+} significantly reduces the distance between Trp326 and Cys193, we checked whether any further enhancement in FRET would occur on addition of ATP. Interestingly, ATP brought the two fluorophores even closer and the *R* for NBD-512 CW4 was reduced by ~6 Å (Fig. 7A; Table 2). ADP, on the other hand, causes a smaller change in distance (~4 Å) between the two (Fig. 7B; Table 2). A similar effect was observed for the catalysis deficient mutant NBD-512 CW4 D327N (Fig. 7C and D; Table 2), further confirming that unlike other ABC transporters, the conserved Asp327 in NBD 512 is not involved in Mg^{2+} coordination nor important for ATP binding [29]. Expectedly, NBD-512 CW4 E238A, which is affected in Mg^{2+} binding, also shows poor conformational change upon ATP/ADP addition (Fig. 6D).

In comparison to ATP, the inability of ADP to further induce FRET emphasizes the role of γ-phosphate in the docking of the substrate. In other words, the presence of Mg–ADP results in a more open conformation for the binding pocket as compared to when the substrate Mg–ATP docks in. Thus, the formation of a functional nucleotide-binding pocket is dictated both by the metal ion as well as by the nucleotide itself.

3.7. Asn328 is a γ-phosphate sensor

How does this nucleotide-binding domain discriminate between ATP and ADP? For this purpose we examined the role of vicinal residues of Trp326 and Cys193. In particular, we were interested in Asn328 that is again unique to N-terminal NBDs of fungal ABC transporters (Fig. 1) and which we have previously shown to be important for the ability of the protein to impart drug resistance to the cell [29].

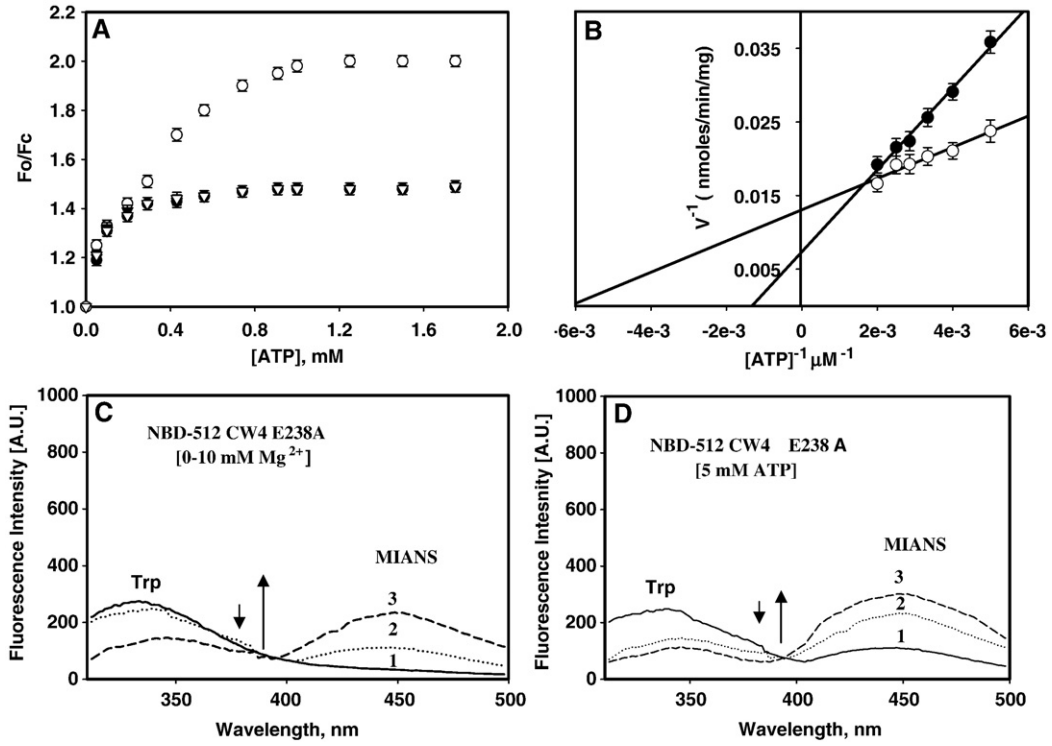

Fig. 6. Functional properties of NBD-512 CW4 E238A. (A) Concentration dependent binding of ATP to the MIANS-labelled NBD-512 CW4 (○) NBD-512 CW4 E238A (●) and NBD-512 E238A (▽) mutant variant. Normalized fluorescence intensity (F_o/F_c) was plotted as a function of ATP concentration, where F_o refers to the fluorescence intensity of the sample in absence of ATP and F_c represents the fluorescence emission intensity at 450 nm upon ATP addition (corrected for dilution). The plot represents averages of three different experiments done in duplicates. The bars represent standard deviations. From the slope and ordinate of the Scatchard plot (plot not shown), dissociation constant (K_d) for ATP binding was determined to be 0.49 ± 0.03 mM for NBD-512 E238A, 0.08 ± 0.04 mM for NBD-512 CW4 and 0.47 ± 0.05 mM for NBD-512 CW4 E238A, assuming a single binding site per molecule. (B) Lineweaver–Burk plots of dependence of ATPase activity of NBD-512 CW4 and NBD-512 CW4 E238A mutant variant on substrate: ATPase assay for NBD-512 CW4 and mutant NBD-512 CW4 E238A at 30 °C for 30 min was carried out using different concentrations of substrate (0–5 mM, as described under Methods). The linear portion of the activity curves was used to obtain Lineweaver–Burk plots of the ATPase activity for NBD-512 CW4 (●) and mutant NBD-512 CW4 E238A (○). For NBD-512 CW4, V_{max} was estimated to be 80.2 ± 6.0 nmol min^{-1} mg $protein^{-1}$ and K_M was 120 ± 4 µM. For NBD-512 CW4 E238A, V_{max} was estimated to be 150.3 ± 4.0 nmol min^{-1} mg $protein^{-1}$ and K_M was 650 ± 15 µM. The data shown is average of three different experiments done in triplicates.(C) Fluorescence emission spectra of MIANS-labelled NBD-512 CW4 E238A mutant variant measured in presence of increasing concentrations of $MgCl_2$ (curve 1, unlabelled protein alone, curve 2, with 8 mM EDTA and no $MgCl_2$; curve 3, 5 mM $MgCl_2$; curve 4, 10 mM $MgCl_2$). (D) Fluorescence emission spectra of MIANS-labelled NBD-512 CW4 E238A mutant variant measured in presence of increasing concentrations of ATP (curve 1 with 8 mM EDTA and no $MgCl_2$; curve 2, 10 mM $MgCl_2$ and No ATP; curve 3, 10 mM $MgCl_2$ and 5 mM ATP). Efficiency of energy transfer was calculated for the change in fluorescence from curve 2 to curve 3 in the former and curves 1 to 3 in the latter case.

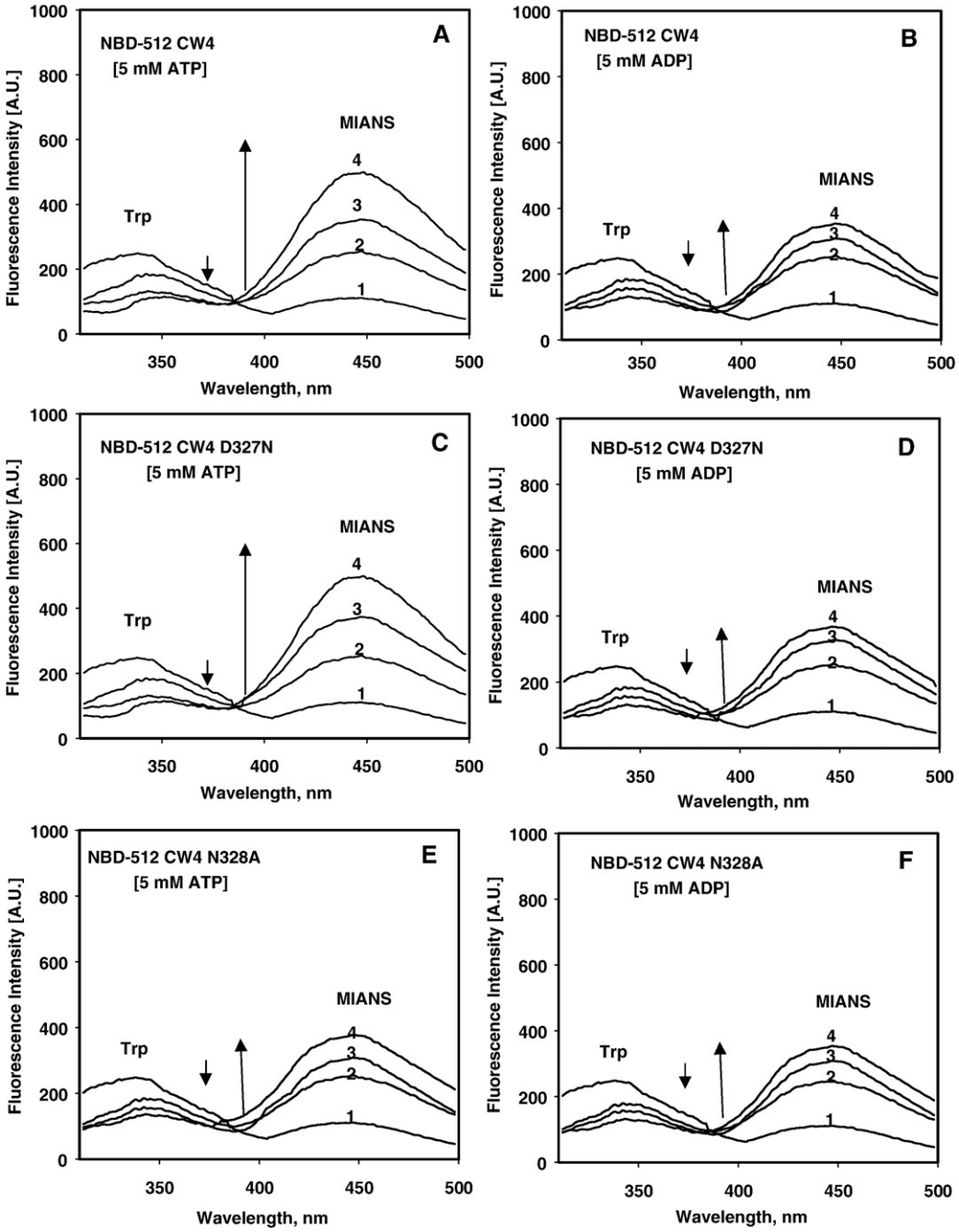

Fig. 7. Effect of ATP/ADP on FRET. Purified 0.4 μM NBD-512 CW4 or mutant variant in ATPase buffer were labelled using 50 μM MIANS for 15 min. After labeling, the samples were titrated with increasing molar fractions of ATP (0–10 mM) and emission spectra were recorded between 310 and 500 nm (slit width 5 nm) upon excitation at 295 nm (slit width 5 nm). (A) Fluorescence emission spectra of MIANS-labelled NBD-512 CW4 mutant variant measured in presence of increasing concentrations of ATP (curve 1 with 8 mM EDTA and no MgCl2, curve 2, 10 mM $MgCl_2$ and no ATP; curve 3, 10 mM $MgCl_2$ and 2.5 mM ATP; curve 4, 10 mM $MgCl_2$ and 5 mM ATP). (B) Fluorescence emission spectra of MIANS-labelled NBD-512 CW4 mutant variant measured in presence of increasing concentrations of ATP (curve 1 with 8 mM EDTA and no $MgCl_2$; curve 2, 10 mM $MgCl_2$ and no ADP; curve 3, 10 mM $MgCl_2$ and 2.5 mM ADP; curve 4, 10 mM $MgCl_2$ and 5 mM ADP). (C) Fluorescence emission spectra of MIANS-labelled NBD-512 CW4 D327N mutant variant measured in presence of increasing concentrations of ATP (curve 1 with 8 mM EDTA and no $MgCl_2$, curve 2, 10 mM $MgCl_2$ and no ATP; curve 3, 10 mM $MgCl_2$ and 3.5 mM ATP; curve 4, 10 mM $MgCl_2$ and 5 mM ATP). (D) Fluorescence emission spectra of MIANS-labelled NBD-512 CW4 D327N mutant variant measured in presence of increasing concentrations of ADP (curve 1 with 8 mM EDTA and no $MgCl_2$; curve 2, 10 mM $MgCl_2$ and no ADP; curve 3, 10 mM $MgCl_2$ and 3.5 mM ADP; curve 4, 10 mM $MgCl_2$ and 5 mM ADP). (E) Fluorescence emission spectra of MIANS-labelled NBD-512 CW4 N328A mutant variant measured in presence of increasing concentrations of ATP (curve 1 with 8 mM EDTA and no $MgCl_2$, curve 2, 10 mM $MgCl_2$ and no ATP; curve 3, 10 mM $MgCl_2$ and 2.5 mM ATP; curve 4, 10 mM $MgCl_2$ and 5 mM ATP). (F) Fluorescence emission spectra of MIANS-labelled NBD-512 CW4 N328A mutant variant measured in presence of increasing concentrations of ADP (curve 1 with 8 mM EDTA and no $MgCl_2$; curve 2, 10 mM $MgCl_2$ and no ADP; curve 3, 10 mM $MgCl_2$ and 2.5 mM ADP; curve 4, 10 mM $MgCl_2$ and 5 mM ADP). Note: In each case efficiency of energy was calculated from curves 1 to 4.

Monitoring the quenching of Trp fluorescence upon the addition of Mg–ATP suggested that NBD-512 N328E or NBD-512 N328A bound Mg–ATP with an affinity similar to NBD-512. So did the mutant variant NBD-512 CW4 N328A [K_d for NBD-512 N328E (0.08 ± 0.01 mM); NBD-512 N328A (0.08 ± 0.01 mM)].

That NBD-512 CW4 N328A continues to bind Mg^{2+} can also be deduced from the *R* value obtained (Table 2). However, unlike NBD-512 CW4, the mutant variant NBD-512 CW4 N328A exhibits a smaller conformation change upon ATP docking (Fig. 7E; Table 2). Indeed, despite proper Mg^{2+} coordination, NBD-512 CW4 N328A does not

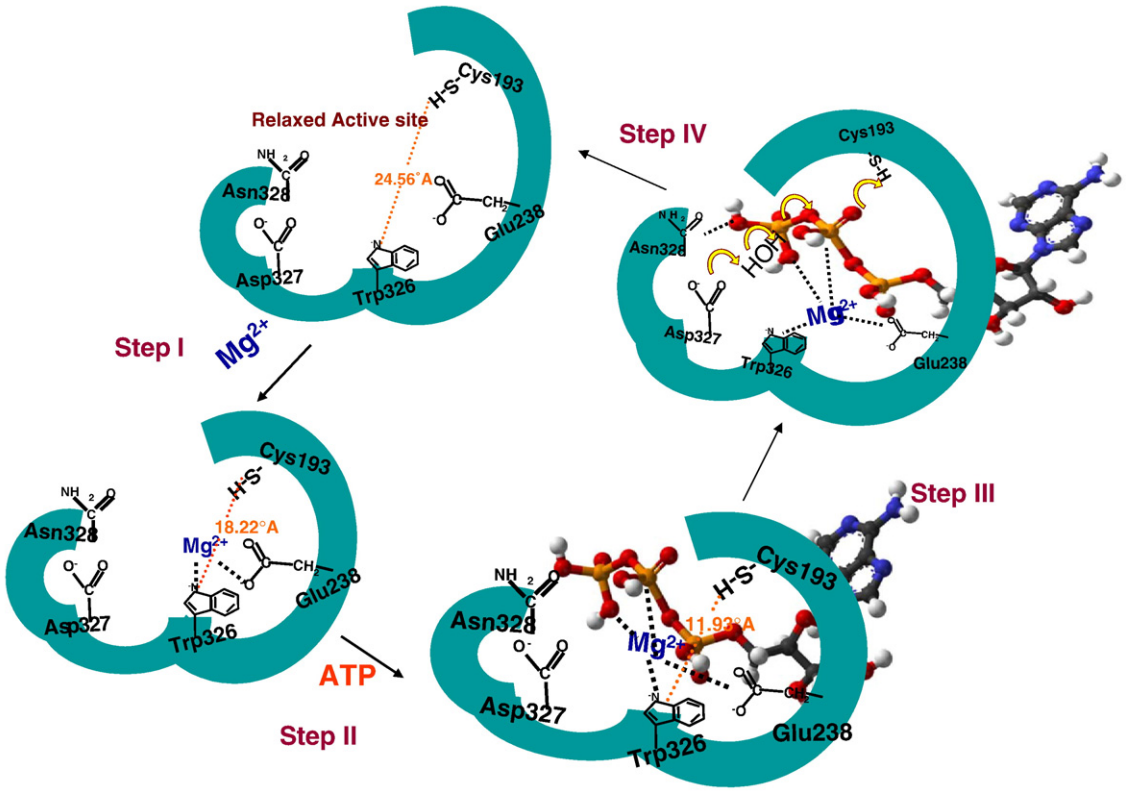

Fig. 8. Hypothetical model for catalytic cycle of N-terminal active site of Cdr1p. Step I: Coordination of Mg^{2+} by Trp326 of the Walker B Motif and Glu238 of Q-loop of NBD-512 induces the first conformational change. Step II: ATP docking and γ-phosphate sensing by Asn328 of the extended Walker B motif of NBD-512 induces the second conformational change. Step III: ATP hydrolysis by the concerted action of Asp327 of Walker B and Cys193 of the Walker A motif. Step IV: Release of phosphate and ADP and active site is relaxed. Note: All the distances mentioned in the figures, tables and text are calculated between MIANS labelled on Cys193 and Trp326 of NBD-512 of Cdr1p.

differentiate between ATP and ADP (Fig. 7E and F; Table 2). This would also explain its inability to hydrolyze ATP. Thus, Asn328 appears to be a sensor of the γ-phosphate of ATP and the subsequent conformational change therefore critical for catalysis.

It may also be pointed out here that a great deal of debate has taken place on the role of the equivalent Glu residue at this position in other ABC transporters that has also been shown to be essential for ATPase activity. It had been suggested that the Glu acts as a general or catalytic base [36]. However, Schmitt et al. have pointed out that this may not be the whole story since converting it to Gln in other ABC transporters led to varying degrees of ATPase activity [36]. We have previously shown that the Asp327 adjacent to Asn328 had taken on the catalytic role reserved for the glutamate in other systems. Our results suggest that Asn328 too has acquired a new role, as a sensor of the γ-phosphate. Given that in NBD-512 several residues have taken on new roles, this is perhaps an extension of this trend.

4. Discussion

Besides demonstrating the essentiality of the two NBDs, we have also shown the functional asymmetry of the two NBDs in Cdr1p [25,37], and unequivocally shown that the unique substitutions in the N-terminal domain have significance for ATP hydrolysis by the domain and to the functioning of the full protein in the cell [26–29]. Using isolated N-terminal NBD (NBD-512) of Cdr1p which probably functions as monomer and making the corresponding mutations in the full protein, we showed that Cys193 in Walker A and Asp327 in Walker B motifs of NBD-512 are both essential for ATP hydrolysis [26,28,29]. Further, we showed that Asp327 could act as a catalytic base since replacement by Asn resulted in interesting pH effects on ATP hydrolysis [29]. ATP binding by NBD-512 requires Mg^{2+} as well as the presence of Trp326 in the Walker B motif of binding pocket [28]. ATP binding to NBD-512 induces a conformation change, which is specific to Mg–ATP docking rather than ATP hydrolysis in the wild type NBD-512 [28]. This was supported by the fact that the catalysis defunct mutant variants, NBD-512 C193A and NBD-512 D327N continued to exhibit conformational change upon ATP binding similar to native NBD-512 [28]. Together these results suggested that the typical residues work in conjunction and contribute physically to the active site formation [26,28,29]. Thus the N-terminal NBD of Cdr1p and, by extension those of other fungal transporters like Pdr5p, have evolved so as to use their unique substitutions to perform the task of ATP binding and hydrolysis [26,28].

In the current study we have attempted to obtain greater mechanistic details of the mechanism of ATP hydrolysis owing to the unusual substitutions within this otherwise conserved domain. By employing FRET, we have resolved the issues related to Mg^{2+} coordination and ATP binding in the N-terminal NBD of Cdr1p. For this purpose, we generated a mutant variant NBD-512 CW4 that had a single Cys (193) and a single Trp (326). We also established that this mutant variant functioned similar to the wild type NBD-512 protein as far as ATP binding and hydrolysis was concerned.

Using this mutant variant, we for the first time confirm that both Mg^{2+} and nucleotide binding contribute to the formation of the active site in the domain. The entry of Mg^{2+} into the active site causes a first large conformational change that brings Trp326 and Cys193 into close proximity. Further, Mg^{2+} has a distinct effect not only on FRET between Trp326 and the MIANS on Cys193, but also causes an enhancement of the intrinsic fluorescence of Trp326 in the mutant variant NBD-512 CW4. Thus Trp326 plays a significant role in Mg^{2+} coordination, which in turn induces a conformational change within the domain. Our FRET results further show that the typically conserved Glu238 of Q-loop of NBD-512, is another residue involved in coordination of the metal ion since its substitution as in NBD-512 CW4 E238A does not allow Trp326

and Cys193 to move sufficiently close in the nucleotide-binding pocket despite the presence of Mg^{2+}. Thus the uniquely placed Glu238, which replaces Gln in the N-terminal NBD of all fungal ABC transporters, takes over the role of Mg^{2+} coordination. On the other hand, the uniquely placed Asn328, which is also common to all fungal transporters, acts primarily as a γ-phosphate sensor and is responsible for the second conformational change that occurs upon ATP binding.

Taken together, one can visualize a three-step mechanism of ATP catalysis at NBD-512. The first step occurs when Mg^{2+} enters the pocket and contacts Trp326 of Walker B and Glu238 of Q-loop (Fig. 8 Step I). This induces a conformational change that drags Cys193 of the Walker A motif towards the catalytic pocket. As a result, Trp326 and Cys193 come within close proximity (R decreases to ~18.2 Å from 24.5 Å). Subsequently, a second conformational change occurs when ATP docks with its phosphates directed towards the pocket. Such a positioning automatically brings the γ-phosphate close to the uniquely placed Asn328 residue in the extended Walker B motif. The sensing of the γ-phosphate by Asn328 is responsible for the second small but significant conformational change in the NBD. As a result Cys193 comes even closer to Trp326 (R ~ 12 Å; Fig. 8 Step II). This sensing of the γ-phosphate and closing in of the Walker A and Walker B motifs towards the substrate constitutes an important event preceding ATP hydrolysis. The third step is the actual catalysis step in which the catalytic residues, Cys193 of Walker A and Asp327 of Walker B, participate (Fig. 8 Step III). Thereafter, the protein has a more open conformation (R is ~14 Å in the presence of Mg–ADP) that allows ADP to leave.

As mentioned earlier, we have previously shown that Asp326 acts as a catalytic base in ATP hydrolysis [29]. In order to understand the role of Cys193 in the catalysis, we generated the mutant variant NBD-512 C193S. In this mutant, Cys was replaced by Ser whose hydroxyl has a higher pK_a than the thiol. At pH 6.5, this mutant variant has ~20% the activity of the wild type protein, NBD-512. However, at pH 8.5 it showed equal if not better ATPase activity as compared to NBD-512, suggesting that the abstraction of the proton too is an essential step in the ATPase activity (Supplementary data Fig. S4A and S4B).

As also deduced from data available for other ATPases [17,33,38], we therefore suggest the following catalytic mechanism: Asp327 acting as a catalytic base abstracts a proton from a water molecule present in the active site as part of the Mg–ATP complex. The hydroxyl ion thus formed attacks at the γ-phosphate allowing the bond between the γ- and β-phosphates to weaken and in turn allowing the β-phosphate to abstract a proton from the –SH of Cys193 (Fig. 8 Step III). The consequence of the proton abstraction is the cleavage of the phosphodiester bond between β- and γ-phosphates, allowing the latter to leave. After ATP is hydrolyzed, the conformation of the active site relaxes back to a more open one since Asn328 cannot sense the β-phosphate of ADP (Fig. 8 Step IV).

The fact that the isolated NBD possesses intrinsic ATPase activity is interesting, particularly in the context of the coordinated functioning of the NBDs in ABC transporters that has been frequently proposed. In Cdr1p too we have reported the asymmetry of the NBDs, suggesting a concerted mechanism of action. How do we account for this apparent disparity? There can be several hypotheses. The isolated domain contains within it all the requisites for intrinsic ATPase activity. However, it is possible that the NBDs show positive cooperativity with respect to ATP hydrolysis when the Signature sequence of one interacts with the ATP bound state of the other. There are several reports to suggest that the conserved Gln in the LSGGQ motif of the second NBD is important for the formation of the catalytic site in the first. Mutational studies in MalK, for example, indicate that this Gln is not a catalytic residue but could 'stimulate' ATPase activity [39]. It is quite likely that ATP docking in the active site is sensed not only by the Asn328 but also perhaps by one or more residues in the LSGGQ motif of the second NBD as shown in the molecular dynamics simulation for MJ7096 [40,41]. It is possible too that this recognition and subsequent conformational change/interdomain interactions are responsible for the positive cooperativity in ATP hydrolysis. Another equally likely scenario is that the accessibility of ATP to the active site of one of the NBDs may be regulated by the other via steric considerations. However when drug binds to Cdr1p, conformational changes in the TM domains are sensed by one of the NBDs and the signal is transduced to the second NBD via the Signature sequence of the former. When ATP is bound/hydrolyzed in this second NBD, it allows the domain to swing out, a conformational change that is transduced to the first NBD via the Signature sequence of the second. Such a sequence of events could also be cooperative and require a concerted action of both NBDs with neither half being capable of functionally replacing the other.

Like the other motifs in the N-terminal NBDs, the ABC signature sequences of Cdr1p and other fungal transporters too appear to have diverged away from that of other ABC transporters. Whether this became necessary to compensate for the substitutions in their N-terminal NBDs or whether they have evolved a new mechanism for coming together for ATP hydrolysis and drug efflux, is a question we are currently examining.

Acknowledgements

The work presented in this paper has been supported in parts by grants from Department of Biotechnology, (DBT/PR3825/Med/14/488 (a)/2003), Council of Scientific and Industrial Research (38(1122)/06/EMR-II), Department of Science and Technology (SR/SO/BB-12/2004), and European Commission, Brussels (QLK2-CT-2001-02377). VR and MG acknowledge the University Grants Commission, India for the support in the form of Senior Research Fellowship.

Appendix A. Supplementary data

Supplementary data associated with this article can be found, in the online version, at doi:10.1016/j.bbamem.2008.04.010.

References

[1] M.I. Borges-Walmsley, K.S. McKeegan, A.R. Walmsley, Structure and function of efflux pumps that confer resistance to drugs, Biochem. J. 376 (2003) 313.
[2] I. Holland, P. Cole, K. Kuchler, C. Higgins, ABC Proteins from Bacteria to Man, Academic Press, San Diego,CA, 2003.
[3] R.A. Calderone, *Candida* and Candidiasis, ASM Press, Washington, DC, 2002.
[4] R. Prasad, S.L. Panwar, Smriti, Drug resistance in yeasts—an emerging scenario, Adv. Microb. Physiol. 46 (2002) 155.
[5] T.C. White, Increased mRNA levels of ERG16, CDR, and MDR1 correlate with increases in azole resistance in *Candida albicans* isolates from a patient infected with human immunodeficiency virus, Antimicrob. Agents Chemother. 41 (1997) 1482.
[6] M.L. Hernaez, C. Gil, J. Pla, C. Nombela, Induced expression of the *Candida albicans* multidrug resistance gene CDR1 in response to fluconazole and other antifungals, Yeast 14 (1998) 517.
[7] D. Sanglard, F. Ischer, M. Monod, J. Bille, Cloning of *Candida albicans* genes conferring resistance to azole antifungal agents: characterization of CDR2, a new multidrug ABC transporter gene, Microbiology 143 (Pt 2) (1997) 405.
[8] T.C. White, K.A. Marr, R.A. Bowden, Clinical, cellular, and molecular factors that contribute to antifungal drug resistance, Clin. Microbiol. Rev. 11 (1998) 382.
[9] V. Gupta, A. Kohli, S. Krishnamurthy, N. Puri, S.A. Aalamgeer, S. Panwar, R. Prasad, Identification of polymorphic mutant alleles of CaMDR1, a major facilitator of *Candida albicans* which confers multidrug resistance, and its in vitro transcriptional activation, Curr. Genet. 34 (1998) 192.
[10] S.S. Pao, I.T. Paulsen, M.H. Saier Jr., Major facilitator superfamily, Microbiol. Mol. Biol. Rev. 62 (1998) 1.
[11] M. Niimi, K. Niimi, Y. Takano, A.R. Holmes, F.J. Fischer, Y. Uehara, R.D. Cannon, Regulated overexpression of CDR1 in *Candida albicans* confers multidrug resistance, J. Antimicrob. Chemother. 54 (2004) 999.
[12] R. Prasad, N. Gupta, M. Gaur, Molecular Basis of Antifungal Resistance, Pathogenic Fungi: Host Interactions and Emerging Strategies for Control, Caister Academic press, England, 2004, pp. 357–414.
[13] J.E. Walker, M. Saraste, M.J. Runswick, N.J. Gay, Distantly related sequences in the alpha- and beta-subunits of ATP synthase, myosin, kinases and other ATP-requiring enzymes and a common nucleotide binding fold, EMBO J. 1 (1982) 945.
[14] R. Prasad, N.A. Gaur, M. Gaur, S.S. Komath, Efflux pumps in drug resistance of *Candida*, Infect. Disord. Drug Targets. 6 (2006) 69.
[15] M. Gao, H.R. Cui, D.W. Loe, C.E. Grant, K.C. Almquist, S.P. Cole, R.G. Deeley, Comparison of the functional characteristics of the nucleotide binding domains of multidrug resistance protein 1, J. Biol. Chem. 275 (2000) 13098.

[16] P.E. Lapinski, R.R. Neubig, M. Raghavan, Walker A lysine mutations of TAP1 and TAP2 interfere with peptide translocation but not peptide binding, J. Biol. Chem. 276 (2001) 7526.
[17] L.W. Hung, I.X. Wang, K. Nikaido, P.Q. Liu, G.F. Ames, S.H. Kim, Crystal structure of the ATP-binding subunit of an ABC transporter, Nature 396 (1998) 703.
[18] P.M. Jones, A.M. George, Subunit interactions in ABC transporters: towards a functional architecture, FEMS Microbiol. Lett. 179 (1999) 187.
[19] C.A. Hrycyna, M. Ramachandra, U.A. Germann, P.W. Cheng, I. Pastan, M.M. Gottesman, Both ATP sites of human P-glycoprotein are essential but not symmetric, Biochemistry 38 (1999) 13887.
[20] I.L. Urbatsch, B. Sankaran, S. Bhagat, A.E. Senior, Both P-glycoprotein nucleotide-binding sites are catalytically active, J. Biol. Chem. 270 (1995) 26956.
[21] G. Szakacs, C. Ozvegy, E. Bakos, B. Sarkadi, A. Varadi, Role of glycine-534 and glycine-1179 of human multidrug resistance protein (MDR1) in drug-mediated control of ATP hydrolysis, Biochem. J. 356 (2001) 71.
[22] I.L. Urbatsch, K. Gimi, S. Wilke-Mounts, A.E. Senior, Investigation of the role of glutamine-471 and glutamine-1114 in the two catalytic sites of P-glycoprotein, Biochemistry 39 (2000) 11921.
[23] Z.E. Sauna, M. Muller, X.H. Peng, S.V. Ambudkar, Importance of the conserved Walker B glutamate residues, 556 and 1201, for the completion of the catalytic cycle of ATP hydrolysis by human P-glycoprotein (ABCB1), Biochemistry 41 (2002) 13989.
[24] A. Decottignies, A. Goffeau, Complete inventory of the yeast ABC proteins, Nat. Genet. 15 (1997) 137.
[25] P. Saini, N.A. Gaur, R. Prasad, Chimeras of the ABC drug transporter Cdr1p reveal functional indispensability of transmembrane domains and nucleotide-binding domains, but transmembrane segment 12 is replaceable with the corresponding homologous region of the non-drug transporter Cdr3p, Microbiology 152 (2006) 1559.
[26] S. Jha, N. Karnani, S.K. Dhar, K. Mukhopadhayay, S. Shukla, P. Saini, G. Mukhopadhayay, R. Prasad, Purification and characterization of the N-terminal nucleotide binding domain of an ABC drug transporter of *Candida albicans*: uncommon cysteine 193 of Walker A is critical for ATP hydrolysis, Biochemistry 42 (2003) 10822.
[27] S. Jha, N. Karnani, A.M. Lynn, R. Prasad, Covalent modification of cysteine 193 impairs ATPase function of nucleotide-binding domain of a *Candida* drug efflux pump, Biochem. Biophys. Res. Commun. 310 (2003) 869.
[28] V. Rai, S. Shukla, S. Jha, S.S. Komath, R. Prasad, Functional characterization of N-terminal nucleotide binding domain (NBD-1) of a major ABC drug transporter Cdr1p of *Candida albicans*: uncommon but conserved Trp326 of Walker B is important for ATP binding, Biochemistry 44 (2005) 6650.
[29] V. Rai, M. Gaur, S. Shukla, S. Shukla, S.V. Ambudkar, S.S. Komath, R. Prasad, Conserved Asp327 of walker B motif in the N-terminal nucleotide binding domain (NBD-1) of Cdr1p of *Candida albicans* has acquired a new role in ATP hydrolysis, Biochemistry 45 (2006) 14726.
[30] Q. Qu, F.J. Sharom, FRET analysis indicates that the two ATPase active sites of the P-glycoprotein multidrug transporter are closely associated, Biochemistry 40 (2001) 1413.
[31] T. Hiratsuka, Spatial proximity of ATP-sensitive tryptophanyl residue(s) and Cys-697 in myosin ATPase, J. Biol. Chem. 267 (1992) 14949.
[32] T. Spande, B. Witkop, Determination of tryptophan content of proteins with N-bromosuccinimide, Methods Enzymol. 11 (1967) 498.
[33] Y.R. Yuan, S. Blecker, O. Martsinkevich, L. Millen, P.J. Thomas, J.F. Hunt, The crystal structure of the MJ0796 ATP-binding cassette. Implications for the structural consequences of ATP hydrolysis in the active site of an ABC transporter, J. Biol. Chem. 276 (2001) 32313.
[34] P.M. Jones, A.M. George, Mechanism of ABC transporters: a molecular dynamics simulation of a well characterized nucleotide-binding subunit, Proc. Natl. Acad. Sci. U. S. A 99 (2002) 12639.
[35] E.O. Oloo, D.P. Tieleman, Conformational transitions induced by the binding of MgATP to the vitamin B12 ATP-binding cassette (ABC) transporter BtuCD, J. Biol. Chem. 279 (2004) 45013.
[36] J. Zaitseva, S. Jenewein, T. Jumpertz, I.B. Holland, L. Schmitt, H662 is the linchpin of ATP hydrolysis in the nucleotide-binding domain of the ABC transporter HlyB, EMBO J. 24 (2005) 1901.
[37] S. Jha, N. Dabas, N. Karnani, P. Saini, R. Prasad, ABC multidrug transporter Cdr1p of *Candida albicans* has divergent nucleotide-binding domains which display functional asymmetry, FEMS Yeast Res. 5 (2004) 63.
[38] L. Schmitt, H. Benabdelhak, M.A. Blight, I.B. Holland, M.T. Stubbs, Crystal structure of the nucleotide-binding domain of the ABC-transporter haemolysin B: identification of a variable region within ABC helical domains, J. Mol. Biol. 330 (2003) 333.
[39] G. Schmees, A. Stein, S. Hunke, H. Landmesser, E. Schneider, Functional consequences of mutations in the conserved 'signature sequence' of the ATP-binding-cassette protein MalK, Eur. J. Biochem. 266 (1999) 420.
[40] P.M. Jones, A.M. George, Nucleotide-dependent allostery within the ABC transporter ATP-binding cassette: a computational study of the MJ0796 dimer, J. Biol. Chem. 282 (2007) 22793.
[41] P.M. Jones, A.M. George, Multidrug resistance in parasites: ABC transporters, P-glycoproteins and molecular modelling, Int. J. Parasitol. 35 (2005) 555.